

## Electronic Supplementary Information

### **Over 17.5% Efficiency Ternary Organic Solar Cells with Enhanced Photon Utilization via a Medium Band Gap Non-Fullerene Acceptor**

*Congcong Cao, †<sup>a</sup> Hanjian Lai, †<sup>a</sup> Hui Chen,<sup>ab</sup> Yulin Zhu,<sup>a</sup> Mingrui Pu,<sup>a</sup> Nan Zheng,<sup>c</sup> and Feng He\*<sup>ad</sup>*

<sup>a</sup> Shenzhen Grubbs Institute and Department of Chemistry, Southern University of Science and Technology, Shenzhen 518055, China E-mail: [huf@sustech.edu.cn](mailto:huf@sustech.edu.cn)

<sup>b</sup> Academy for Advanced Interdisciplinary Studies, Southern University of Science and Technology, Shenzhen 518055, China

<sup>c</sup> Institute of Polymer Optoelectronic Materials and Devices, State Key Laboratory of Luminescent Materials and Devices, South China University of Technology, Guangzhou 510640, China

<sup>d</sup> Guangdong Provincial Key Laboratory of Catalysis, Southern University of Science and Technology, Shenzhen, 518055, China

†These authors contributed equally to this work.

## Materials and Methods

**Materials.** All the other chemicals were purchased as reagent grade from J&K, Energy, Macklin, or Sigma-Aldrich, and used without further purification. All solvents for reactions were distilled immediately prior to use.

**Characterization of acceptors.**  $^1\text{H}$  NMR spectra were recorded on a Bruker AV 400 MHz spectrometer in  $\text{CDCl}_3$  with tetramethylsilane (TMS) as an internal standard. UV-Vis absorption spectra of neat and blend films were recorded on a Shimadzu UV3600 spectrometer. Cyclic voltammetry (CV) measurements were done on a CHI 660E potentiostat/galvanostat (Shanghai Chenhua Instrumental Co., Ltd. China) in a solution in acetonitrile of  $0.1 \text{ mol}\cdot\text{L}^{-1}$  tetrabutylammonium hexafluorophosphate ( $\text{Bu}_4\text{NPF}_6$ ) at a potential scan rate of  $100 \text{ mV s}^{-1}$  with  $\text{Ag}/\text{Ag}^+$ , platinum wire and glassy carbon disk as reference electrode, counter electrode and working electrode under an argon atmosphere, to determine the HOMO and LUMO levels of the polymers.

**Device fabrication and characterization.** Devices were fabricated with the conventional structure of ITO/PEDOT:PSS/active layer/PNDIT-F3N/Ag. At first, the ITO substrates were ultrasonic cleaned with acetone, detergent, deionized water and isopropanol sequentially, followed by drying at  $90 \text{ }^\circ\text{C}$  in a vacuum oven for 12h. The ITO substrates were UV-treated for 15 min, and the PEDOT:PSS interlayer from a precursor solution was spin-coated onto the ITO substrate, then heated at  $150 \text{ }^\circ\text{C}$  for 15 min. The substrates were transferred to a glovebox, and the active layer was spin-coated from  $16 \text{ mg/mL}$  chloroform solution (D:A = 1:1.2, 0.5% CN) at 3000 rpm for

45 seconds. Then thermal annealing at 100 °C for 10 min was performed to optimize the morphology of active layer. The proportion of BTIC-Th2Br-EH in the total acceptors was 15%, the others conditions were same to the those of binary devices. Subsequently, the electron transporting layer of PNDIT-F3N (0.5 mg/mL in methanol) was spin-coated at 2000 rpm for 35 seconds on the films. Later, Ag electrodes with were deposited by thermal evaporation on the top of devices for about 100 nm in a vacuum chamber.

The binary and ternary devices were tested in a nitrogen-filled glovebox at room temperature. Steady-state current-voltage ( $J$ - $V$ ) curves were measured by a Keithley 2400 source-measurement unit under AM 1.5 G spectrum from a solar simulator (Enlitech, Inc) calibrated by a silicon reference cell (Hamamatsu S1133 color, with KG-5 visible filter). The external quantum efficiency (EQE) was measured by a solar cell photodetector measurement system (Enlitech, Inc). The mobilities of hole and electron were measured by the field-independent space charge limited current (SCLC) method. The structures of hole-only and electron-only devices were ITO/PEDOT:PSS/activelayer/MoO<sub>3</sub>/Ag and ITO/ZnO/activelayer/PNDIT-F3N/Al, respectively. The mobility was determined by fitting the current-bias characteristics in the dark to the model of a single carrier SCLC following the Mott-Gurney law

$$J = \frac{9}{8} \varepsilon_0 \varepsilon_r \mu \frac{V^2}{L^3}$$

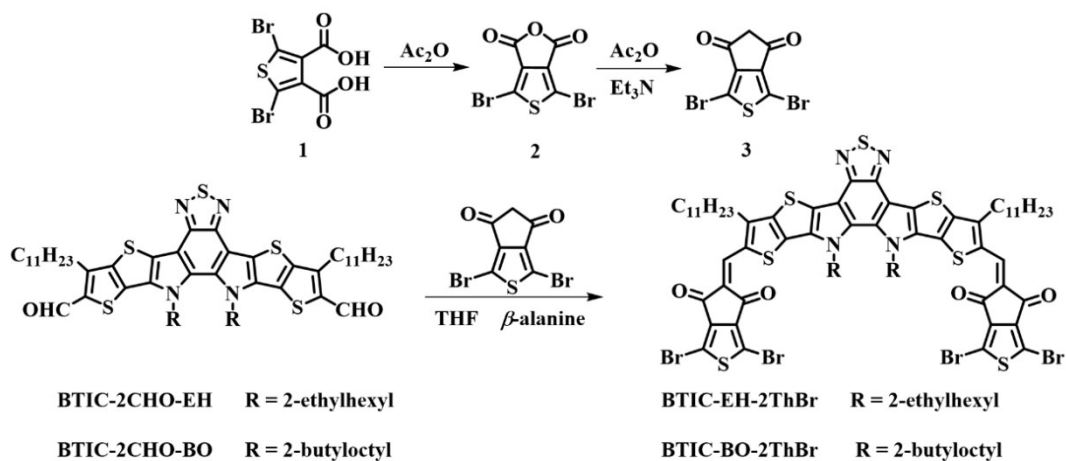
where  $J$  is the measured current density,  $\mu$  is the carrier mobility,  $\varepsilon_0$  is the permittivity of free space ( $8.85419 \times 10^{-12}$  CV<sup>-1</sup> m<sup>-1</sup>),  $\varepsilon_r$  is the average dielectric constant of

material,  $L$  is the thickness of the active layer, and  $V$  is the applied voltage. The carrier mobility was calculated from the slope of the  $J^{1/2} - V$  curves.

**Energy loss measurement.** Highly sensitive EQE was measured through an integrated system with Fourier transform photocurrent meter (PECT-600, Enlitech). EQE<sub>EL</sub> measurement was performed from 0 to 2.5 V by high sensitivity solar cell electroluminescence (EL) efficiency measurement system (REPS, Enlitech). The spectrometer covers 300~1100 nm, including the luminescence efficiency measurement from nearultraviolet, visible and near-infrared. The detail calculation of energy loss according to following equation:

$$\begin{aligned}
 E_{loss} &= E_g - qV_{OC} = (E_g - qV_{OC}^{SQ}) + (qV_{OC}^{SQ} - qV_{OC}^{rad}) + (q\Delta V_{OC}^{rad} - qV_{OC}) \\
 &= (E_g - qV_{OC}^{SQ}) + q\Delta V_{OC}^{rad, belowgap} + q\Delta V_{OC}^{non-rad} \\
 &= \Delta E_1 + \Delta E_2 + \Delta E_3
 \end{aligned}$$

**Characterization of morphology.** Grazing incident wide-angle X-ray scattering (GIWAXS) measurements were carried out at the 8ID-E beam line with the Advanced Photon Source (APS), Argonne National Laboratory using x-rays with a wavelength of  $\lambda = 1.1385 \text{ \AA}$  and a beam size of 200  $\mu\text{m}$  (h) and 20  $\mu\text{m}$  (v). A 2-D PILATUS 1M-F detector was used to capture the scattering patterns and was situated 208.7 mm from samples. Atom force microscopy (AFM) images were performed on a Veeco Metrology Group/Digital Instruments. Transmission electron microscopy (TEM) images were performed using a HITACHI H-7650 electron microscope operating at an acceleration voltage of 100 kV.



**Scheme S1.** The synthetic routes of BTIC-EH-2ThBr and BTIC-BO-2ThBr.

## Experimental section

**Compound 2:** 5g of compound 1 was added to a 250 ml round bottom flask, 100 ml acetic anhydride was added, and the mixture was stirred overnight at 110 °C. The temperature was lowered to room temperature (rt), and after removal of the solvent, the crude product was directly reacted in the next step without further processing.

**Compound 3:** The crude compound 2 was added to a 250 ml round bottom flask, 60ml acetic anhydride and 30 ml triethylamine were added, respectively. After stirring for 10 min, 5ml of ethyl acetoacetate was added. The mixture was stirred for 12 h at rt, and then the mixture was poured into the mixture of concentrated HCl (20 ml) and ice-water (60 ml). After heating to 60 °C for 1 h, the temperature was lowered to rt and filtered, then it was purified by flash column chromatography with CHCl<sub>3</sub> as eluent to obtain a powder (3.2 g, 68.1% in two steps). <sup>1</sup>H NMR (400 MHz, CDCl<sub>3</sub>) δ: 3.51 (s, 2H).

**Compound BTIC-EH-2ThBr:** A mixture of BT-2CHO-EH (80 mg, 0.078 mmol), compound 3 (123 mg, 0.397 mmol), in CH<sub>2</sub>ClCH<sub>2</sub>Cl/□-alanine/CH<sub>3</sub>OH (30 ml/20

mg/5 ml) was refluxed for 24 h under argon. The reaction mixture was then cooled to rt and then extracted with  $\text{CHCl}_3$ . The organic layer was washed with brine and dried over  $\text{MgSO}_4$ . The crude product was purified by flash column chromatography with  $\text{CHCl}_3$  as eluent and further purified with cycling preparative HPLC to get the product (40 mg, 31.8%).  $^1\text{H NMR}$  (400 MHz,  $\text{CDCl}_3$ )  $\delta$ : 8.24 (s, 2H), 4.75 (m, 4H), 3.19 (m, 4H), 2.08 (m, 2H), 1.86-1.90 (m, 4H), 1.44-1.50 (m, 4H), 1.37 (m, 4H), 1.26-1.28 (m, 24H), 1.16-1.17 (m, 4H), 0.97-1.02 (m, 12H), 0.85-0.88 (t, 6H), 0.64-0.73 (m, 12H).

**Compound BTIC-BO-2ThBr:** A mixture of BT-2CHO-BO (50 mg, 0.044 mmol), compound 3 (68.2 mg, 0.22 mmol), in  $\text{CH}_2\text{ClCH}_2\text{Cl}/\square\text{-alanine}/\text{CH}_3\text{OH}$  (30 ml/20 mg/5 ml) was refluxed for 24 h under argon. The reaction mixture was then cooled to rt and extracted with  $\text{CHCl}_3$ . The organic layer was washed with brine and dried over  $\text{MgSO}_4$ . The crude product was purified by flash column chromatography with  $\text{CHCl}_3$  as eluent and further purified with cycling preparative HPLC to get the product (20 mg, 26.4%).  $^1\text{H NMR}$  (400 MHz,  $\text{CDCl}_3$ )  $\delta$ : 8.20 (s, 2H), 4.74-4.76 (m, 4H), 3.17-3.21 (m, 4H), 2.13-2.16 (m, 2H), 1.85-1.89 (m, 4H), 1.43-1.49 (m, 4H), 1.33-1.39 (m, 4H), 1.25-1.30 (m, 28H), 0.99-1.18 (m, 12H), 0.84-0.97 (m, 22H), 0.61-0.72 (m, 12H).

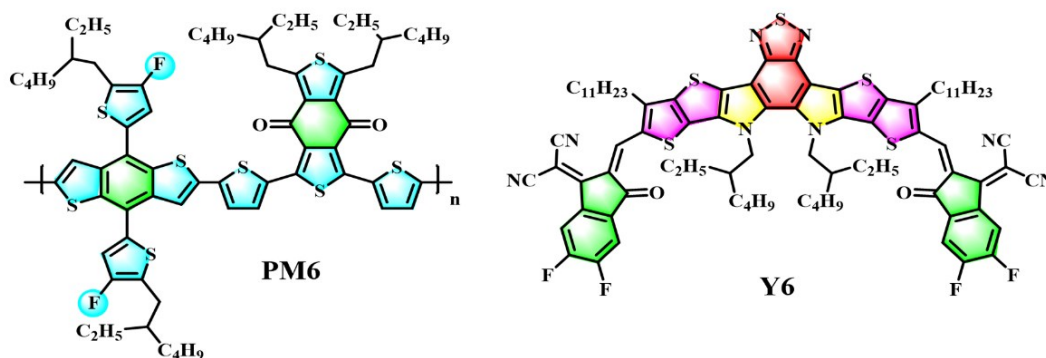


**Figure S1.** The chemical structures of PM6, Y6.

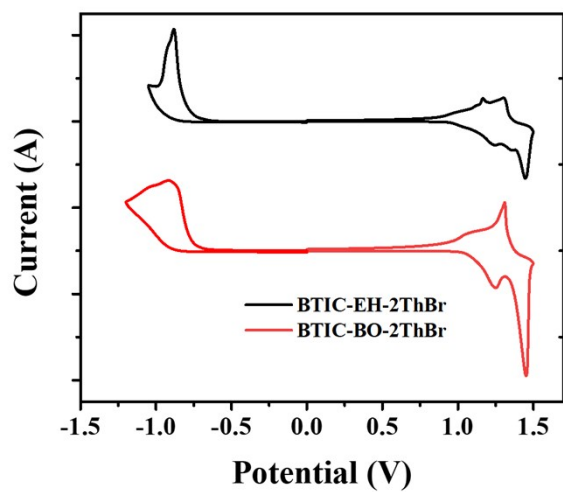


**Figure S2.** Cyclic voltammetry curves of the films of BTIC-EH-2ThBr and BTIC-BO-2ThBr.

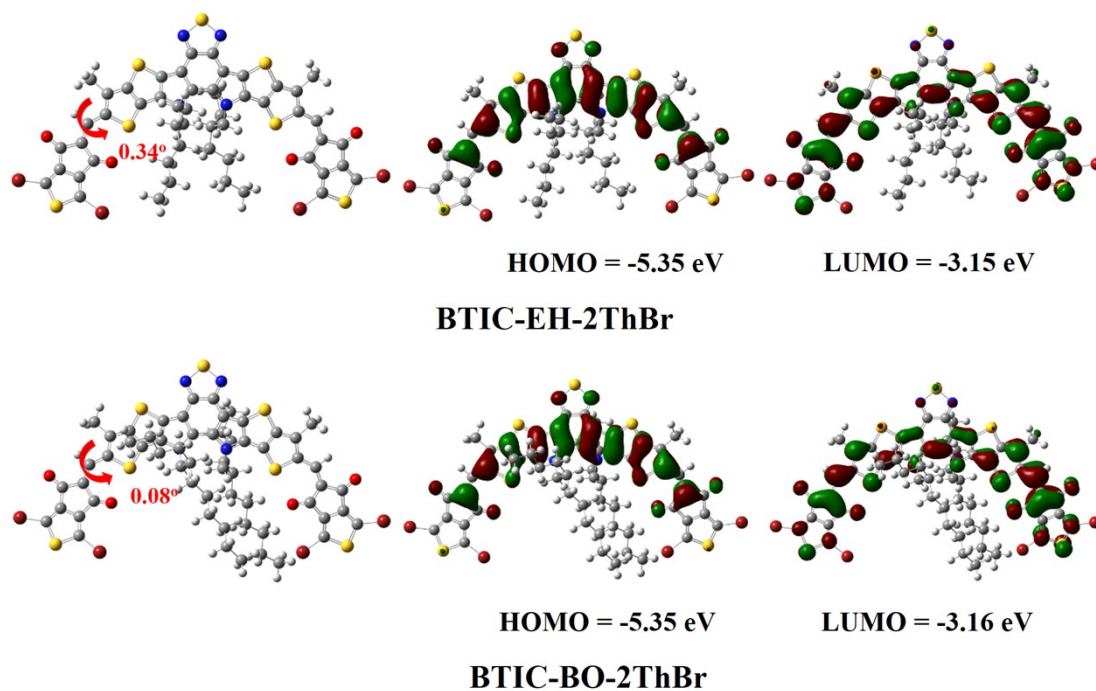


**Figure S3.** Optimized molecular geometry in the top view, torsional angles, frontier molecular distributions, and the corresponding energy levels of BTIC-EH-2ThBr and BTIC-BO-2ThBr using DFT calculations at the B3LYP/6-31g\*(d, p) level.

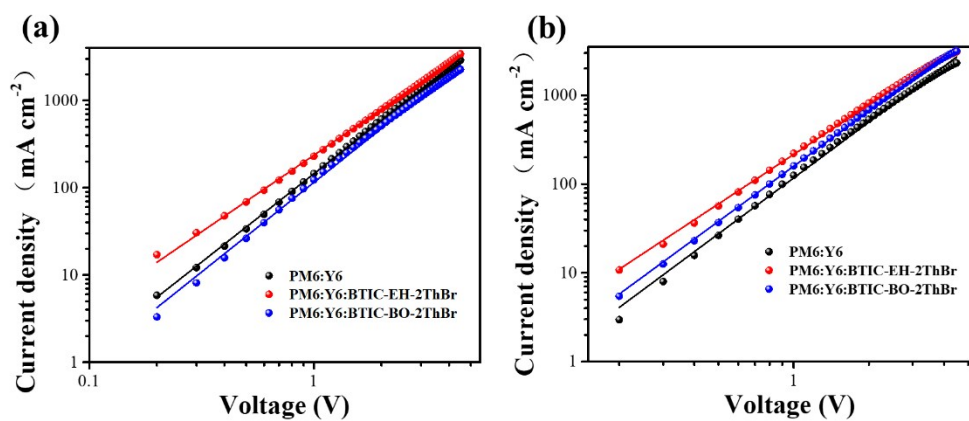


**Figure S4.** (a)  $J$ - $V$  curves of the hole-only devices. (b)  $J$ - $V$  curves of the electron-only devices.



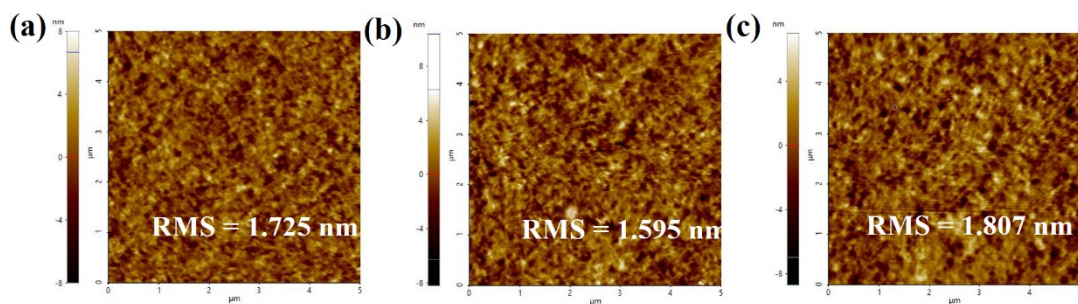


**Figure S5.** AFM height images of (a) PM6:Y6, (b) PM6:Y6:BTIC-EH-2ThBr and (c) PM6:Y6:BTIC-BO-2ThBr.

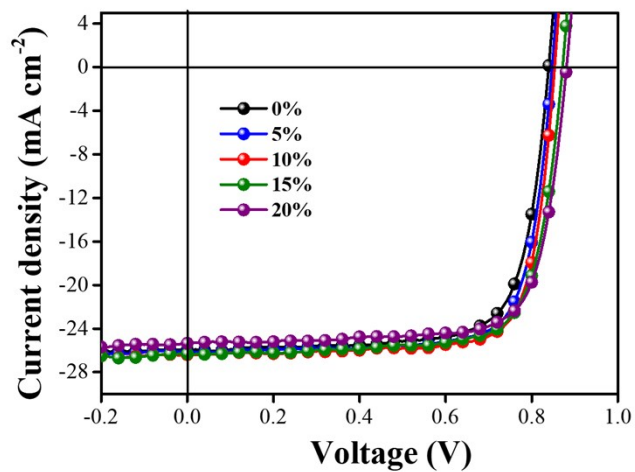


**Figure S6.**  $J$ - $V$  curves of ternary OPVs based on PM6:Y6:BTIC-EH-2ThBr blend films with various BTIC-EH-2ThBr weight ratios in the acceptor mixture.

**Table S1.** SCLC mobilities of the blend films.

Devices	Hole ( $\mu_h$ ) Mobilities ( $\text{cm}^2 \text{V}^{-1} \text{s}^{-1}$ )	Eletron ( $\mu_e$ ) Mobilities ( $\text{cm}^2 \text{V}^{-1} \text{s}^{-1}$ )	$\mu_e/\mu_h$
PM6:Y6	$3.10 \times 10^{-4}$	$4.98 \times 10^{-4}$	1.61
PM6:Y6: BTIC-EH-2ThBr	$5.42 \times 10^{-4}$	$7.58 \times 10^{-4}$	1.40
PM6: Y6: BTIC-BO-2ThBr	$3.61 \times 10^{-4}$	$5.91 \times 10^{-4}$	1.64

**Table S2.** Detailed energy loss of binary and ternary devices.

Devices	$E_g$ (eV)	$qV_{oc}$ (eV)	$E_{loss}$ (eV)	$\Delta E_1$ (eV)	$\Delta E_2$ (eV)	$\Delta E_3$ (eV)
PM6:Y6	1.412	0.840	0.572	0.255	0.071	0.250
PM6: BTIC-EH-2ThBr	1.410	0.853	0.557	0.255	0.071	0.231
PM6: BTIC-BO-2ThBr	1.420	0.851	0.569	0.260	0.072	0.236

**Table S3.** Photovoltaic performance of ternary solar cells with BTIC-EH-2ThBr as the third component.

BTIC-EH-2ThBr ratio <sup>a</sup>	$V_{oc}$ (V)	$J_{sc}$ ( $\text{mA cm}^{-2}$ )	FF (%)	PCE <sup>b</sup> (%)
0%	0.840	25.92	75.13	16.35 (16.12)
5%	0.847	26.18	76.88	17.05 (16.91)
10%	0.853	26.39	77.90	17.54 (17.35)
15%	0.872	26.31	75.72	17.37 (17.08)
20%	0.881	25.35	76.33	17.05 (16.88)

<sup>a</sup> Various weight ratios of BTIC-EH-2ThBr in the acceptor mixture (total donor/acceptor ratio is kept as 1:1.2). <sup>b</sup> The average of 10 devices.

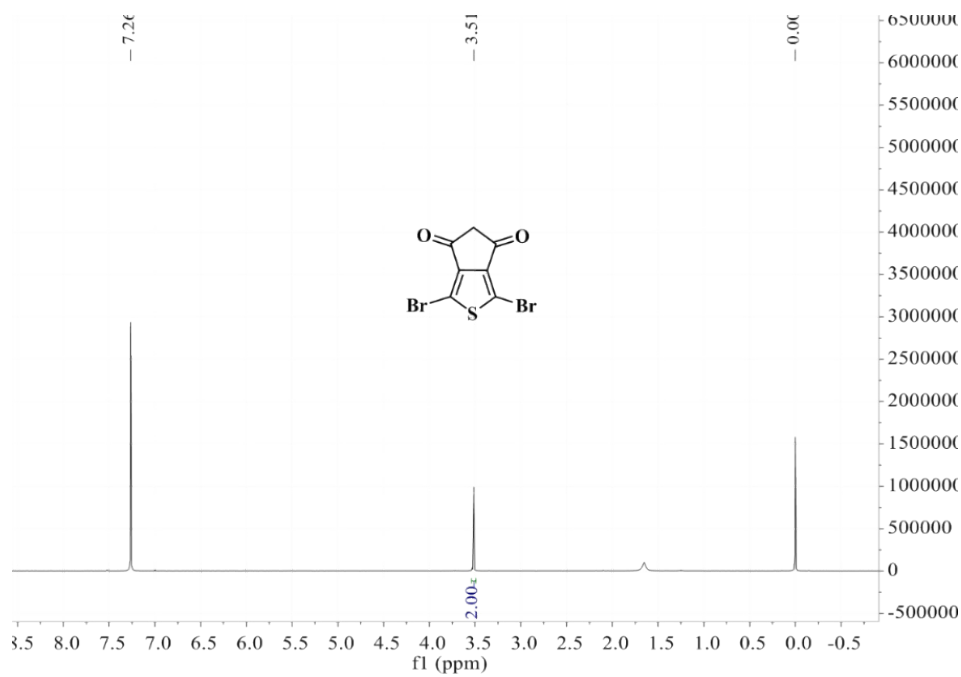


Figure S7.  $^1\text{H}$  NMR of Compound 3 in  $\text{CDCl}_3$ .

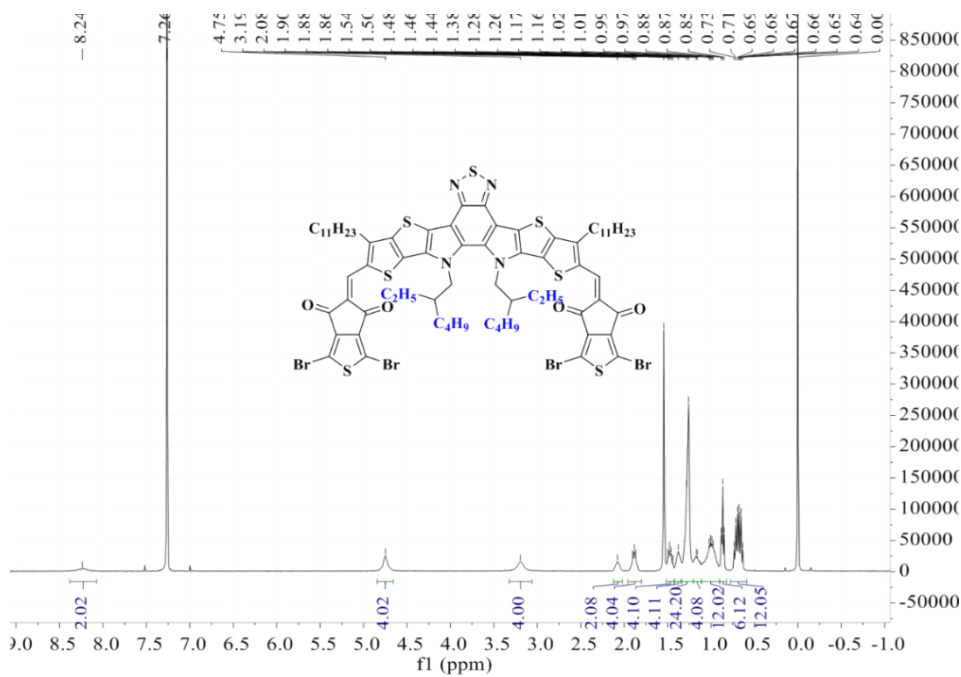
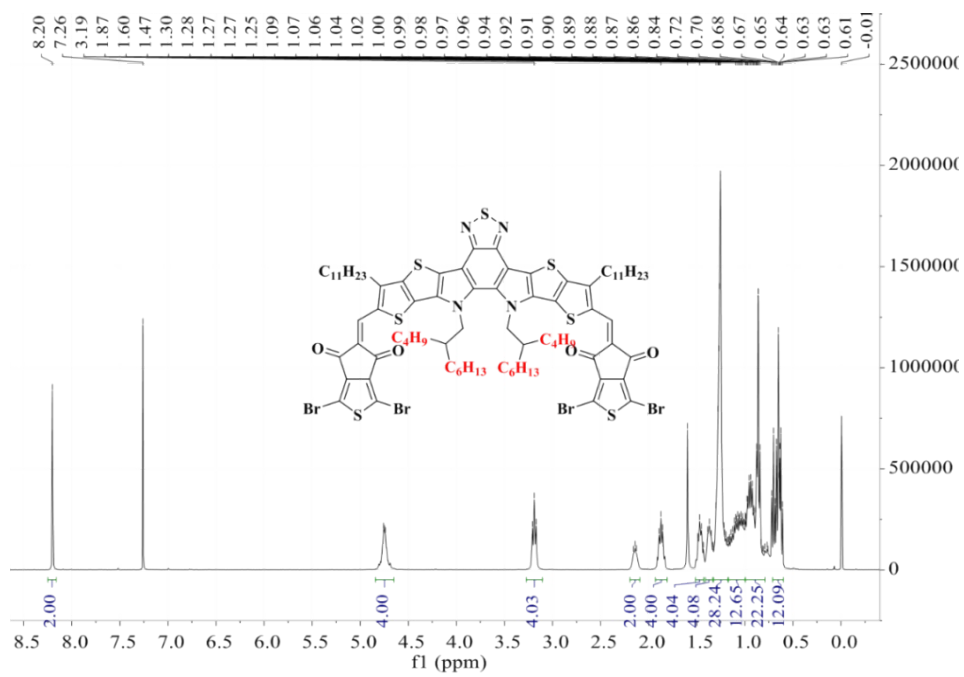


Figure S8.  $^1\text{H}$  NMR of BTIC-EH-2ThBr in  $\text{CDCl}_3$ .



**Figure S9.**  $^1\text{H}$  NMR of BTIC-BO-2ThBr in  $\text{CDCl}_3$ .